

Phenomenology of the Little Higgs model with X-Parity

A. FREITAS¹, P. SCHWALLER², D. WYLER²

¹ *Department of Physics & Astronomy, University of Pittsburgh,
3941 O'Hara St, Pittsburgh, PA 15260, USA*

² *Institut für Theoretische Physik, Universität Zürich,
Winterthurerstrasse 190, CH-8057 Zürich, Switzerland*

Abstract

In the popular littlest Higgs model, T-parity can be broken by Wess-Zumino-Witten (WZW) terms induced by a strongly coupled UV completion. On the other hand, certain models with multiple scalar multiplets (called moose models) permit the implementation of an exchange symmetry (X-parity) such that it is not broken by the WZW terms. Here we present a concrete and realistic construction of such a model. The little Higgs model with X-Parity is a concrete and realistic implementation of this idea. In this contribution, the properties of the model are reviewed and the collider phenomenology is discussed in some detail. We also present new results on the decay properties and LHC signatures of the light triplet scalars that are predicted by this model.

1 THE LITTLE HIGGS AND T-PARITY

Little Higgs models [1] can naturally explain a relatively large hierarchy between the electroweak scale and a fundamental symmetry breaking scale that is several orders of magnitude larger, $\Lambda \sim 10$ TeV. In these models, the Higgs boson is a Goldstone boson of a spontaneously broken global symmetry. In order to construct realistic models with a non-trivial Higgs potential and fermion Yukawa couplings, the global symmetry needs to be broken explicitly, and thus can only be an approximate symmetry. Nevertheless, if each of these explicit breaking terms keeps a subgroup of the global symmetry unbroken, a Higgs mass term is only generated beyond one-loop order and thus can naturally be small.

Little Higgs models predict additional particles with masses at an intermediate scale $f \sim 1$ TeV. These new particles lead to large tree-level corrections to electroweak precision observables [2], which rule out values of f below several TeV. However, the introduction of a discrete symmetry called T-parity [3, 4] forbids the dangerous tree-level diagrams. As a result, models with T-parity are in agreement with precision data for values of f even below 1 TeV [5]. Moreover, the lightest T-odd particle would be stable and thus could be a candidate for dark matter.

In Ref. [6] it was argued that this picture is not complete, but that a Wess-Zumino-Witten (WZW) term [7] should be added to the Lagrangian of the model. WZW terms typically occur if the symmetry breaking at the scale Λ is facilitated by some strong dynamics. As was shown in Ref. [6], this WZW term would be odd under T-parity, leading to the decay of the lightest T-odd particle [8]. However, recently it was shown that a parity can be implemented in a different way such that it leaves the WZW term invariant [9]. In this approach

the discrete symmetry, which will be named X-parity henceforth, is defined as a exchange symmetry between two scalar fields. This idea has been worked out into a complete and realistic model [10], called the minimal moose model with X-parity. In this contribution, the properties of the model will be reviewed and the collider phenomenology will be discussed in some detail. We also present new results on the decay properties and LHC signatures of the light triplet scalars that are predicted by this model.

2 THE MODEL

The model is constructed as an effective theory valid up to the cutoff scale $\Lambda \sim 10$ TeV. At this scale some unspecified new physics is assumed to be responsible for the fundamental symmetry breaking and for a renormalizable completion of the theory. The model is based on a $[SU(3)_L \times SU(3)_R]^4$ global symmetry, which is spontaneously broken to the diagonal subgroup $SU(3)^4$ by the fundamental symmetry-breaking mechanism. As a result, four copies of a non-linear sigma model appear, $X_i = e^{2ix_i/f}$, $i = 1, 2, 3, 4$. Under the global symmetry they transform as

$$X_{1,3} \rightarrow L_{1,3} X_{1,3} R_{1,3}^\dagger, \quad X_{2,4} \rightarrow R_{2,4} X_{2,4} L_{2,4}^\dagger, \quad (1)$$

which can be interpreted as the $X_{1,3}$ and $X_{2,4}$ having “opposite directions” in a moose diagram. The scalar sector, defined in this way, is invariant under the exchange symmetry

$$SU(3)_L \leftrightarrow SU(3)_R, \quad X_1 \leftrightarrow X_2, \quad X_3 \leftrightarrow X_4. \quad (2)$$

This symmetry will be called X-parity in the following. It has the remarkable feature that it leaves the WZW term invariant [9], so that the X-parity is an exact symmetry and the lightest X-odd particle is stable. The symmetry structure and the effect of X-parity is depicted in terms of a moose diagram in Fig. 1.

In order to construct a complete model, a $[SU(2) \times U(1)]_L \times [SU(2) \times U(1)]_R$ subgroup is gauged, resulting in a set of heavy X-odd gauge bosons with masses of order $f \sim 1$ TeV and a set of massless X-even gauge bosons that are identified with the Standard Model (SM) gauge bosons. The scalar Lagrangian is given by

$$\mathcal{L}_G = \frac{f^2}{4} \sum_{i=1}^4 \text{tr}[(D_\mu X_i)(D^\mu X_i)^\dagger], \quad \text{with} \quad \begin{aligned} D_\mu X_{1,3} &= \partial_\mu X_{1,3} - iA_{L\mu} X_{1,3} + iX_{1,3} A_{R\mu}, \\ D_\mu X_{2,4} &= \partial_\mu X_{2,4} - iA_{R\mu} X_{2,4} + iX_{2,4} A_{L\mu}. \end{aligned}$$

Under X-parity the gauge fields transform as $A_L \leftrightarrow A_R$.

To implement X-parity in the fermion sector, we introduce two left-handed fermion doublets for each fermion flavor, illustrated here for the quark sector. They are embedded into incomplete representations of $SU(3)$ as follows

$$Q_a = (d_a, u_a, 0)^\top, \quad Q_b = (d_b, u_b, 0)^\top.$$

Under the global $SU(3)_L \times SU(3)_R$ group they transform as $Q_a \rightarrow L_i Q_a$ and $Q_b \rightarrow R_i Q_b$, while X-parity interchanges the two fields, $Q_a \leftrightarrow Q_b$. The kinetic terms for these fermions

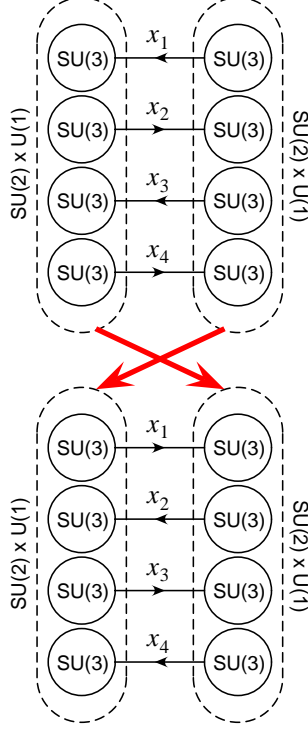


Figure 1: Illustration of the global and gauge symmetry structure of the model. The difference between the upper and the lower diagram and the red arrows indicate the effect of X-parity.

assume the standard form. Under X-parity, they decompose into the X-even standard model fermions and their X-odd partners, the mirror fermions, denoted by Q_H . They can be given an $\mathcal{O}(f)$ Dirac mass by the following parity invariant mass term:

$$\mathcal{L}_M = -\frac{\lambda_c}{\sqrt{2}} f \left(Q_a \xi_1 Q_c^c - Q_b \Omega \xi_1^\dagger Q_c^c - Q_b \xi_2 \Omega Q_c^c + Q_a \Omega \xi_2^\dagger \Omega Q_c^c \right) + \text{h.c.}$$

This term introduces the righthanded partners $Q_c^c = (d_c^c, u_c^c, 0)^T$ for the X-odd fermions Q_H and $\xi_i = \sqrt{X_i} = e^{ix_i/f}$.

The Yukawa couplings of the light quarks and leptons are small and therefore don't lead to large contributions to the Higgs mass through radiative corrections. This is however not true for the top quark and therefore the top quark Yukawa coupling requires special attention. To not explicitly break the global symmetries, the third family doublets have to be embedded into complete $SU(3)$ triplets by adding a third vector-like quark:

$$Q_{3a} = (d_{3a}, u_{3a}, U_a)^\top, \quad Q_{3b} = (d_{3b}, u_{3b}, U_b)^\top, \quad Q_{3c}^c = (d_{3c}^c, u_{3c}^c, U_c^c)^\top.$$

The top Yukawa coupling now is given by

$$\mathcal{L}_t = -\lambda f Q_{3a} (X_3 + \Omega X_4^\dagger \Omega) \begin{pmatrix} 0 \\ 0 \\ U_b^c \end{pmatrix} - \lambda f Q_{3b} (\Omega X_3^\dagger \Omega + X_4) \begin{pmatrix} 0 \\ 0 \\ U_a^c \end{pmatrix} + \text{h.c.},$$

where we have introduced two additional singlets U_a^c, U_b^c that transform as $U_a^c \leftrightarrow U_b^c$ under X-parity, and the X-even combination of which will form the right-handed component of the top quark.

In total the top quark has three partners, two of which are X-odd, and one being X-even. The ratio $R = \lambda/\lambda_c$ of the two top Yukawa couplings is a free parameter of the model.

3 MASS SPECTRUM

All X-odd partners of the standard model fermions have $\mathcal{O}(f)$ masses whose precise values are determined by the parameter λ_c . An exception is the top-quark sector, where we have in total four states, two X-even and two X-odd fermions. While both X-odd fields obtain $\mathcal{O}(f)$ masses, the X-even fields mix to give the physical top-quark that remains massless before EWSB and an additional T -quark with a mass of $\mathcal{O}(f)$. The mixing in the top sector is determined by a single parameter $R = \lambda/\lambda_c$ that is the ratio of the top Yukawa coupling and the mirror fermion mass parameter.

The masses of the X-odd gauge bosons are fixed once the symmetry breaking scale f is specified. If $\lambda_c \sim \mathcal{O}(1)$, the X-odd partner of the hypercharge boson, A_H , is always the lightest heavy gauge boson, which can serve as a dark matter candidate.

The scalar pseudo-Goldstone fields can be decomposed into SU(2) gauge multiplets as follows:

$$x_i = \begin{pmatrix} \phi_i + \eta_i/\sqrt{12} & h_i/2 \\ h_i^\dagger/2 & -\eta_i/\sqrt{3} \end{pmatrix}, \quad (3)$$

where $\phi_i = \phi_i^a \sigma^a/2$ are SU(2) triplets, h_i are complex doublets, and η_i are real singlets. The explicit partial breaking of the global symmetry through the Higgs self-interaction, the gauge interactions, the mirror fermion kinetic and mass terms, and the top Yukawa coupling generate masses for all of these scalar particles at the one- and two-loop level. These loop contributions are divergent and depend on the cut-off scale Λ of the effective theory. Nevertheless, the order of magnitude of the mass parameters can be estimated parametrically, leading to $\mathcal{O}(f) \sim \mathcal{O}(1 \text{ TeV})$ masses for almost all scalars. Only one X-even triplet, called ϕ_a , and one X-even doublet obtain masses of the order of the electroweak scale, $\mathcal{O}(100 \text{ GeV})$.

The light doublet will form the SM-like “little” Higgs boson. Together with the second, heavy X-even doublet, the structure of the Higgs potential is similar to a Two-Higgs-Doublet model. However, mixing between the two X-even doublets is suppressed by their mass ratio $\mathcal{O}(100 \text{ GeV})^2/\mathcal{O}(1 \text{ TeV})^2$. Nevertheless, mixing effects could lead to interesting consequences, since they have been shown to necessarily lead to CP violation [10].

Table 1 summarizes the particle content beyond the SM fermions and gauge bosons. Also indicated in the table are the quantum numbers of these fields with respect to the X-parity. Note that the present model is very similar to the older moose model proposed in Ref. [4]. As a result, the original T-parity proposed by Cheng and Low [4] is also respected by our model on the classical level, although it is broken by the WZW term as explained above. However, since the WZW term is the only source of T-parity breaking, T-parity is still a good quantum number for most production and decay processes, and therefore it is also listed in Tab. 1.

As mentioned above, the particle spectrum cannot be predicted precisely due to the dependence on the unknown UV physics at the scale Λ . Within the framework of the

Table 1: Particle content of the minimal moose model with X-parity (besides SM fermions and gauge bosons). Also listed is the even-/oddness of the particles under X- and T-parity.

Field		X-parity	T-parity
Heavy gauge bosons	$B_H^0, W_H^{0,\pm}$	—	—
Singlet scalars	η_x	—	—
	η_a, η_b	+	—
Triplet scalars	ϕ_x	—	—
	ϕ_a, ϕ_b	+	—
X-odd doublets	h_{H1}, h_{H2}	—	+
X-even doublets	h^0, H^0, A^0, H^\pm	+	+
Mirror leptons	L_H	—	—
Mirror quarks	Q_H	—	—
Top partners	T_H, T'	—	—
	T	+	+

effective theory, the UV completion will generate counterterms that cancel the divergence of the loop corrections to the mass parameters. Setting all unknown coefficients of the finite parts of these counterterms to one, the estimates for the mass patterns in Fig. 2 are obtained, for two choices of the Yukawa ratio R .

For $\mathcal{O}(1)$ values of the unknown counterterm coefficients, the lightest X-odd particle is the heavy U(1) gauge boson B_H^0 . Since it is weakly interacting and stable it is a viable dark matter candidate.

Note that the SM-like Higgs boson h^0 and the X-even scalar triplet ϕ_a are not shown in Fig. 2, since they have masses of the order of the electroweak scale, as mentioned above, and thus are much lighter than the other new particles.

4 ELECTROWEAK PRECISION CONSTRAINTS

To estimate the effect of the new particles on the electroweak precision constraints, we calculate the leading contributions to the T-parameter. An important positive contribution to T comes from the custodial symmetry violating $|h^\dagger D_\mu h|^2$ operators that are contained in the kinetic term for the Goldstone fields. This is partially cancelled by a negative contribution from the mass splitting between the X-odd gauge bosons W_H^\pm and W_H^0 and by a contribution from the Higgs sector of the model that can be either positive or negative, both appearing at the one-loop level. The mixing in the top sector leads to a contribution of similar size at one loop that strongly depends on the parameter R .

All contributions to T are suppressed by the scale f and essentially decouple for $f \geq 2$ TeV. Lower values of f are viable provided some moderate cancellations happen. Figure 3 shows the allowed region in the $f - R$ plane with all other parameters fixed. We see that

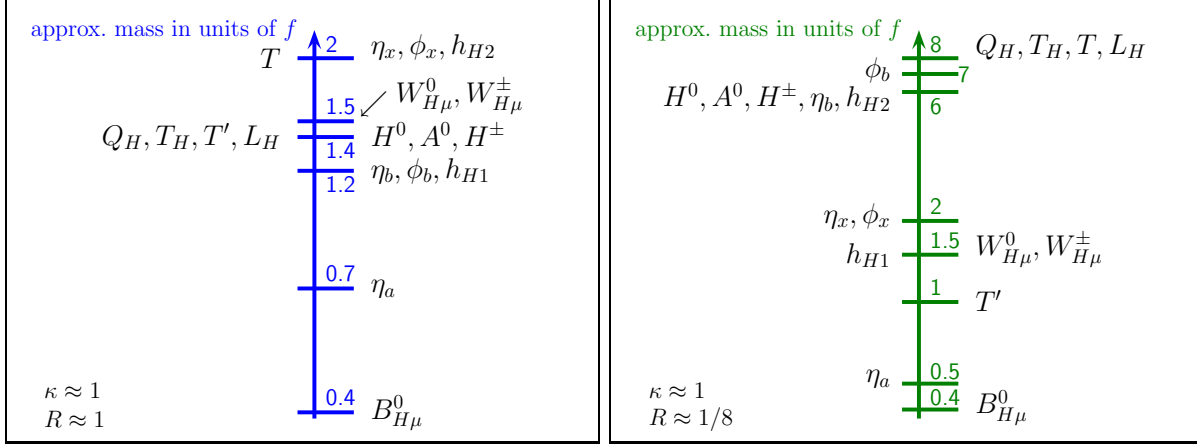


Figure 2: Approximate patterns of two typical mass spectra for heavy new particles.

values of f down to the TeV scale and slightly below are possible, making the model testable at the LHC.

5 COLLIDER PHENOMENOLOGY

Due to the exact realization of X-parity, X-odd particles can be produced only in pairs at colliders. They then decay in cascades that eventually end with the lightest X-odd particle, the B_H^0 boson. Assuming $f \sim 1$ TeV, most of the new particles are within reach of the Large Hadron Collider (LHC), but separation of the small signals from the background is difficult in many cases.

For instance, the heavy SU(2) gauge bosons $W_H^{0,\pm}$ are predicted to be much heavier than the lighter B_H^0 boson, and since they only have electroweak couplings, their production cross sections are relatively small [11]. The same is true for most of the heavy scalar particles with $\mathcal{O}(f) \sim \mathcal{O}(\text{TeV})$ masses.

Relatively large cross sections are expected for the colored particles. In particular, the X-even top partner T can be produced singly. Single T production, $pp \rightarrow T\bar{b} + X$, $\bar{T}b + X$ proceeds dominantly through the partonic processes $b\bar{q} \rightarrow T\bar{q}'$ and $\bar{b}q \rightarrow \bar{T}q'$, where q, q' are SM quarks of the first two generations. The requirement of bottom quarks in the initial state, originating from the parton distribution function of the proton, leads to a suppression of the single production process, so that pair production through $gg \rightarrow T\bar{T}$ and $q\bar{q} \rightarrow T\bar{T}$ can be competitive. The LHC production cross sections are shown in Fig. 4.

The single T production cross section depends sensitively on the mixing between the ordinary top quark t and the heavy T quark, and thus on the parameter $R \equiv \lambda_1/\lambda_2$. On the other hand, the pair production process is mainly mediated through QCD interactions and therefore insensitive to the mixing parameters. In spite of the suppression, the single production process is dominant for $M_T \gtrsim 1$ TeV.

The T quark can decay into Higgs bosons via the top Yukawa couplings or into the B_H^0 boson via its gauge coupling. The branching ratios are shown in Fig. 5. For most of the parameter space the channel $T \rightarrow h^0 t$ is dominant. If the h^0 Higgs boson is light, and thus

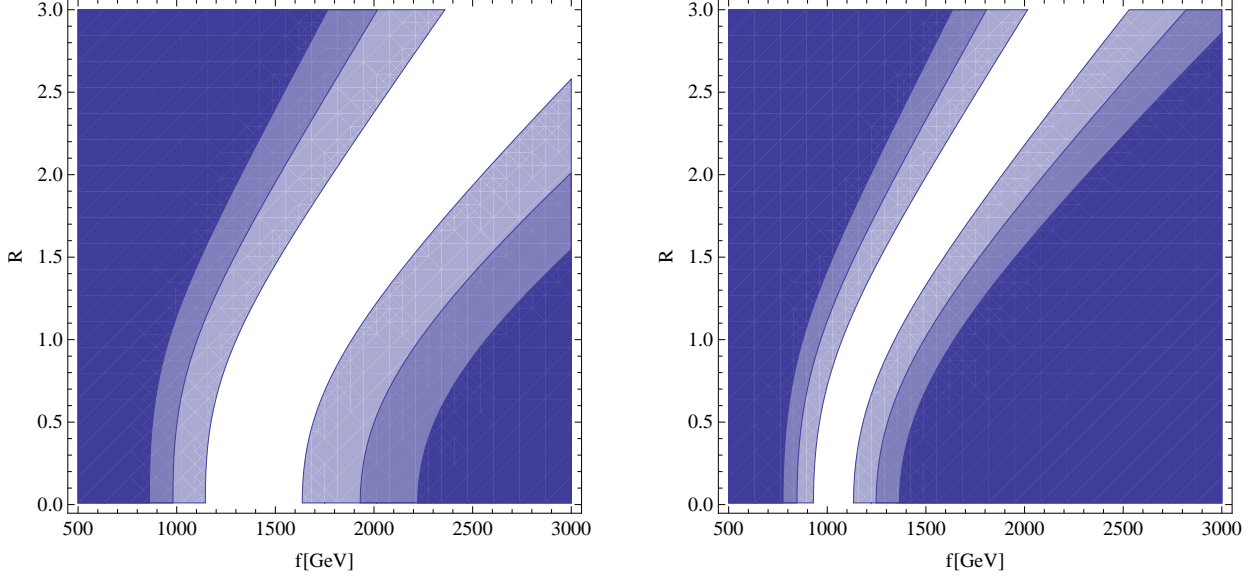


Figure 3: Allowed regions in the $f - R$ plane where the T-parameter agrees with the experimental value. In the left plot we use $\delta_{\pm}^2 = 0.1f^2$ and $\delta_0^2 = 0.2f^2$ while the right plot uses $\delta_{\pm}^2 = -0.15f^2$ and $\delta_0^2 = -0.3f^2$, see [10] for details.

mainly decays via $h^0 \rightarrow b\bar{b}$, the single T mode leads to a final state signature of $4b + W$. The separation of this signal from the SM background will rely heavily on b-tagging and requires a dedicated analysis.

However, the X-odd mirror quarks will be even more difficult to detect at the LHC. They are produced only in pairs, so that the cross sections are smaller than for the T quark. Furthermore, due to the large mass of the SU(2) gauge bosons $W_H^{0,\pm}$, mirror quarks decay directly to the lightest X-odd particle via $Q_H \rightarrow q B_H^0$ for $R \sim \mathcal{O}(1)$. This leads to a very difficult signature with two hard jets and missing energy, which allows discovery only for relatively low mirror quark masses [14]. For small values of R , the mirror quarks become heavier than the SU(2) gauge bosons $W_H^{0,\pm}$, but in this case their production cross section is also very small.

The most promising signal of an X-odd quark is expected from the additional top quark partner T' , since it is predicted to be relatively light¹. As can be seen from Fig. 6, the pair production cross section for $pp \rightarrow T'\bar{T}'$ is sizable and can reach several 100 fb for $\mathcal{O}(\text{TeV})$ masses of the T' . However, the decay signature $T'\bar{T}' \rightarrow t\bar{t} B_H^0 B_H^0$ is very similar to $t\bar{t}$ production in the SM, so that a careful analysis is needed to disentangle signal from background [15].

In contrast, very striking and clean signatures are expected from the production of the scalar triplet ϕ_a . In this model, $\phi_a^{0,\pm}$ is predicted to be relatively light, with a mass that is about one order of magnitude below the scale f . Therefore the production cross sections for the members of this triplet can be relatively large. Since the triplet $\phi_a^{0,\pm}$ is even under

¹Note that it is the T' that cancels the quadratic divergences from top quark loops to the Higgs mass parameter, and therefore its relatively low mass is of central importance for the naturalness of the model.

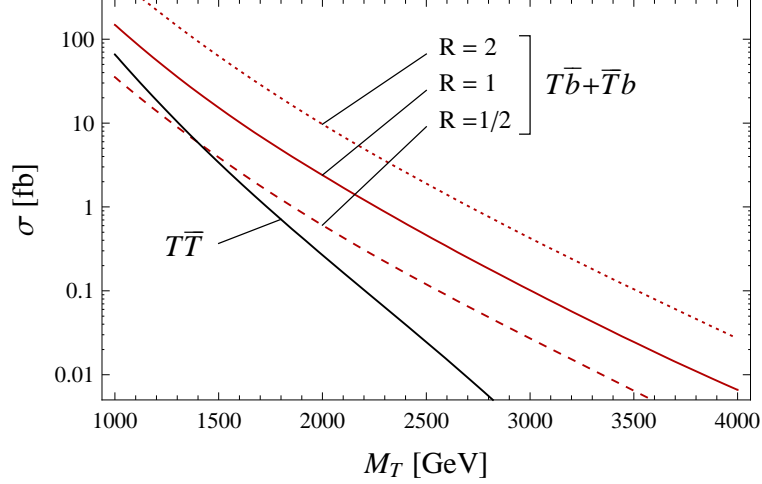


Figure 4: LHC cross sections for single T and $T\bar{T}$ production, as a function of the T quark mass, and for different values of $R \equiv \lambda_1/\lambda_2$. The QCD and factorization scales have been set to M_T , and the center-of-mass energy is $\sqrt{s} = 14$ TeV.

X-parity, but odd under T-parity, it decays through the WZW term into SM gauge bosons:

$$\phi_a^0 \rightarrow ZZ, \gamma\gamma, \gamma Z, \quad (4)$$

$$\phi_a^\pm \rightarrow W^\pm Z, W^\pm \gamma. \quad (5)$$

Electroweak symmetry breaking can induce a small mass splitting between the neutral and charged components of ϕ_a . This mass splitting cannot be calculated reliably since it can receive contributions from higher-dimension operators induced by the UV completion. Nevertheless, the leading contribution to the mass splitting can be parametrically estimated to be of the order $\mathcal{O}[g^4 f^2/(4\pi^2)] \sim \mathcal{O}[g^4 v^2]$. If we assume that ϕ_a^\pm is heavier than ϕ_a^0 this opens up the additional decay channel $\phi_a^\pm \rightarrow (W^\pm)^* \phi_a^0$ through a virtual W boson.

The left plot in figure 7 shows the branching fractions of the different decay modes as a function of the mass splitting between ϕ_a^\pm and ϕ_a^0 . Once the mass difference becomes larger than 15 GeV the decays of ϕ_a^\pm through a virtual W^\pm will dominate over the WZW-term induced decays. The neutral ϕ_a^0 dominantly decays into pairs of photons but also has sizeable branching fractions into the γZ and ZZ channels above the respective thresholds, as can be seen from the right plot in figure 7. Note that the decay into W^+W^- is absent because the WZW term vanishes for the corresponding anomaly-free SU(2) subgroup.

At the LHC, $\phi_a^{0,\pm}$ are mainly produced in pairs through Drell-Yan-type processes with the Feynman diagrams shown in Fig. 8. Since the WZW term is suppressed by several powers of v/f , single production of ϕ_a^0 or ϕ_a^\pm is completely negligible. Furthermore, production of ϕ_a pairs through gluon fusion, which first occurs at one-loop level, is also very small. Fig. 8 shows the tree-level Drell-Yan production cross sections, computed with the program COMPHEP 4.4 [12], using a model file generated with the help of the LAMHEP package [13].

As evident from the figure, the largest cross section is obtained for mixed pair production $pp \rightarrow \phi_a^0 \phi_a^\pm$. Therefore striking signals involving a W boson and several photons are expected

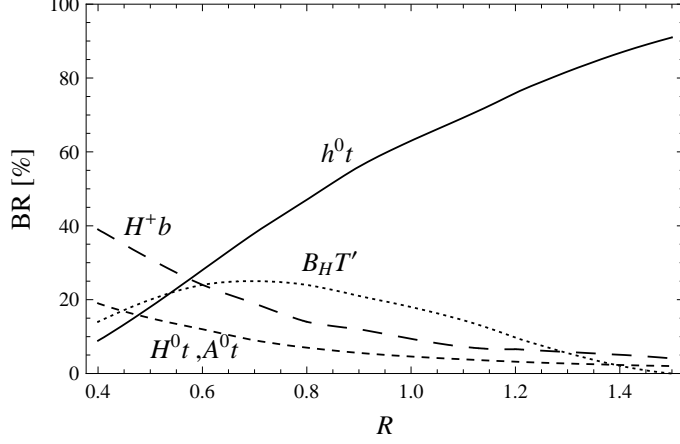


Figure 5: Branching ratio of the heavy X-even T quark, as a function of the ratio $R = \lambda_1/\lambda_2$ of top Yukawa couplings.

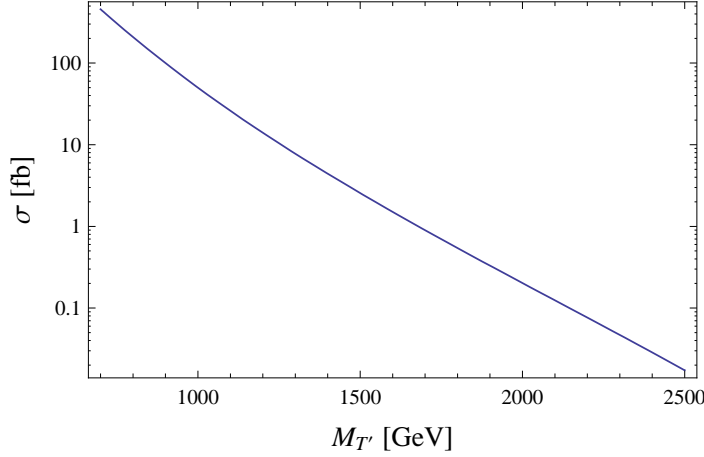


Figure 6: LHC cross section for $T'\bar{T}'$ production, as a function of the T' mass. The QCD and factorization scales have been set to $M_{T'}$, and the center-of-mass energy is $\sqrt{s} = 14$ TeV.

as a unique signature of this process, with very little background from SM processes.

In table 2 we show the signal rates for the most promising detection channels at the LHC involving charged leptons. We assume a mass $m_a = 300$ GeV, which is well beyond any direct detection bounds from the Tevatron², and consider both the cases of small and large mass splitting between ϕ_a^+ and ϕ_a^0 . We require at least one charged lepton in the final state from the leptonic decay of the W^+ . Events with three charged leptons are obtained from leptonic decays of a Z boson appearing either in the decays of ϕ_a^0 or ϕ_a^+ , while the events with two charged leptons come from decays of $\phi_a^+\phi_a^-$ pairs, where both W bosons decay leptonically. All channels are very clean and essentially free of standard model backgrounds, therefore these signals could be observed with a few fb^{-1} at the LHC, provided that instrumental backgrounds are under control.

²The total production cross section for ϕ_a triplets at the Tevatron is less than 1 fb in this case.

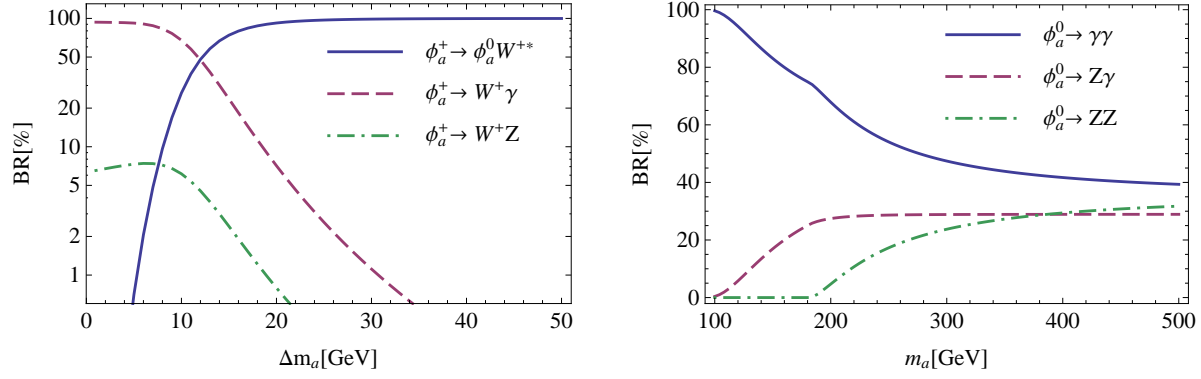


Figure 7: Left plot: Branching fractions of ϕ_a^+ as a function of the mass splitting Δm_a . Right plot: Branching fractions of ϕ_a^0 depending on the mass m_a .

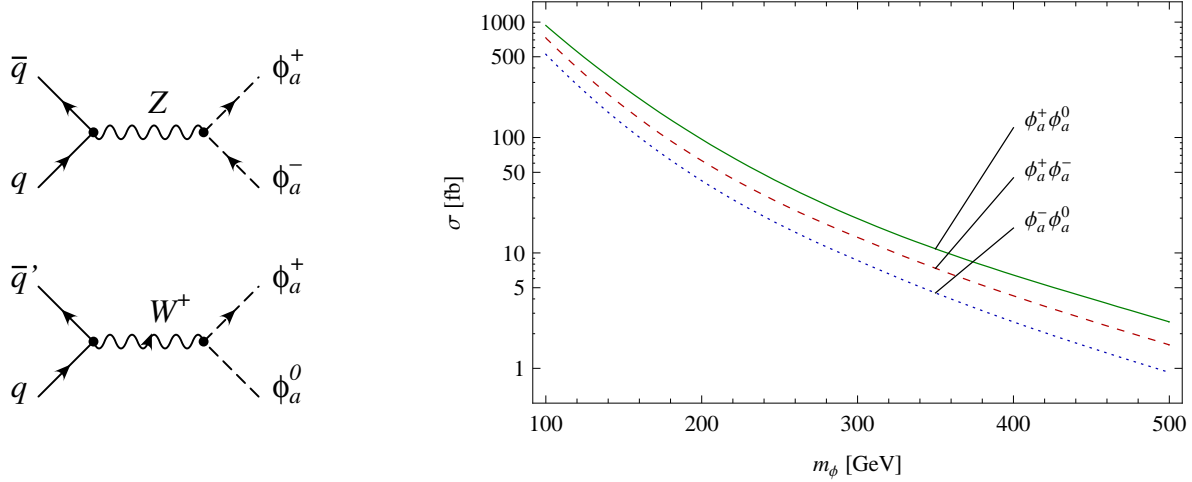


Figure 8: Pair production diagrams and LHC cross sections for the particles in the lightest scalar triplet, as a function of their mass. The factorization scale has been chosen equal to m_ϕ , and the center-of-mass energy is $\sqrt{s} = 14$ TeV.

$\Delta m_a = 5$ GeV	10 TeV	14 TeV	$\Delta m_a = 20$ GeV	10 TeV	14 TeV
$l^+ \gamma \gamma \gamma \cancel{E}$	1.04 fb	1.86 fb	$l^+ \gamma \gamma \gamma \cancel{E}$	0.47 fb	0.84 fb
$l^+ l^+ l^- \gamma \gamma \cancel{E}$	0.049 fb	0.087 fb	$l^+ l^+ l^- \gamma \gamma \cancel{E}$	0.038 fb	0.068 fb
$l^+ l^- \gamma \gamma \cancel{E}$	0.27 fb	0.51 fb	$l^+ l^- \gamma \gamma \gamma \cancel{E}$	0.053 fb	0.10 fb

Table 2: Signal rates for decays of $\phi_a^+ \phi_a^0$ and $\phi_a^+ \phi_a^-$ pairs produced at LHC with 10 TeV and 14 TeV center of mass energy respectively. l^\pm denotes either an electron or a muon.

$\Delta m_a = 5 \text{ GeV}$	10 TeV	14 TeV	$\Delta m_a = 20 \text{ GeV}$	10 TeV	14 TeV
$\gamma\gamma + X$	17.5 fb	32.5 fb	$\gamma\gamma + X$	15.1 fb	28.2 fb
$\gamma\gamma\gamma + X$	6.82 fb	12.6 fb	$\gamma\gamma\gamma + X$	9.31 fb	17.4 fb
			$\gamma\gamma\gamma\gamma + X$	4.20 fb	7.87 fb

Table 3: Multi-photon signals from decays of $\phi_a^+\phi_a^0$ and $\phi_a^+\phi_a^-$ pairs produced at LHC with 10 TeV and 14 TeV center of mass energy respectively.

A large reduction of the signal rates occurs due to requiring leptonic decays of the W or Z bosons. An alternative strategy could be to focus only on photons to identify these signals. In table 3 we present the signal rates for events with more than two, three and four photons in the final state.

The two-photon signal is most challenging to separate from the continuous standard model di-photon background, as is well known from Higgs searches in this channel. If possible at all, this would require an excellent mass resolution to identify the $\phi_a^0 \rightarrow \gamma\gamma$ peak in the invariant mass spectrum, and a rather high luminosity. Requiring a third photon in the final state significantly reduces the standard model background. Here the most important contributions are direct tri-photon production and events with jets or electrons misidentified as photons. Assuming that the instrumental backgrounds can be sufficiently suppressed, this channel has potential for an early discovery at the LHC with only a few fb^{-1} .

6 SUMMARY

The implementation of an exact parity in a little Higgs model is an attractive possibility to ensure good agreement with electroweak data and to yield a viable dark matter candidate. Following an idea by Krohn and Yavin, a realistic model has been constructed that has an unbroken parity realized as an exchange symmetry. It has been shown that this model is in agreement with electroweak precision data and naturally accommodates electroweak symmetry breaking at a scale of the order of 100 GeV.

In this contribution the collider phenomenology and possible discovery of the model at the Large Hadron Collider (LHC) has been analyzed in detail. It was found that many particles with reach of the LHC are predicted, but discovery is challenging for many channels due to low cross sections and signatures with large backgrounds. The most promising signal stems from the production of light parity-even $\text{SU}(2)$ triplet scalars, which have masses near the electroweak scale. These triplet scalars decay into pairs of Standard Model gauge bosons, leading to striking signatures involving multiple photons and leptons from W and Z bosons.

A few open questions remain for further study. While the heavy $\text{U}(1)$ gauge boson B_H^0 is a promising dark matter candidate with the correct quantum numbers, it remains to be checked whether the observed relic dark matter density could be obtained within this model. Furthermore, for successful electroweak symmetry breaking, the Higgs potential must contain a complex parameter, which might lead to potentially observable CP violating effects. The CP violating parameter could also play a role for electroweak baryogenesis.

REFERENCES

- [1] N. Arkani-Hamed, A. G. Cohen and H. Georgi, Phys. Lett. B 513, 232 (2001); N. Arkani-Hamed, A. G. Cohen, E. Katz, A. E. Nelson, T. Gregoire and J. G. Wacker, JHEP 0208, 021 (2002).
- [2] C. Kilic and R. Mahbubani, JHEP 0407, 013 (2004).
- [3] H. C. Cheng and I. Low, JHEP 0309, 051 (2003).
- [4] H. C. Cheng and I. Low, JHEP 0408, 061 (2004).
- [5] J. Hubisz, P. Meade, A. Noble and M. Perelstein, JHEP 0601, 135 (2006).
- [6] C. T. Hill and R. J. Hill, Phys. Rev. D 75, 115009 (2007); Phys. Rev. D 76, 115014 (2007).
- [7] J. Wess and B. Zumino, Phys. Lett. B 37, 95 (1971); E. Witten, Nucl. Phys. B 223, 422 (1983); O. Kaymakcalan, S. Rajeev and J. Schechter, Phys. Rev. D 30, 594 (1984).
- [8] V. Barger, W. Y. Keung and Y. Gao, Phys. Lett. B 655, 228 (2007); A. Freitas, P. Schwaller and D. Wyler, JHEP 0809, 013 (2008).
- [9] D. Krohn and I. Yavin, JHEP 0806, 092 (2008).
- [10] A. Freitas, P. Schwaller and D. Wyler, JHEP **0912**, 027 (2009).
- [11] J. Hubisz and P. Meade, Phys. Rev. D 71, 035016 (2005); A. Freitas and D. Wyler, JHEP 0611, 061 (2006); A. Belyaev, C. R. Chen, K. Tobe and C. P. Yuan, Phys. Rev. D 74, 115020 (2006).
- [12] E. Boos *et al.* [CompHEP Collaboration], Nucl. Instrum. Meth. A 534, 250 (2004).
- [13] A. Semenov, Comput. Phys. Commun. 180, 431 (2009).
- [14] M. S. Carena, J. Hubisz, M. Perelstein and P. Verdier, Phys. Rev. D 75, 091701 (2007).
- [15] T. Han, R. Mahbubani, D. G. E. Walker and L. T. E. Wang, JHEP **0905**, 117 (2009).